

AD-A250 021



2

TECHNICAL REPORT BRL-TR-3338

# BRL

THE EFFECT OF YAW CARDS ON  
THE PITCHING AND YAWING MOTION  
OF SYMMETRIC PROJECTILES

ROBERT L. McCOY

MAY 1992

DTIC  
ELECTE  
MAY 15 1992  
S B D

APPROVED FOR PUBLIC RELEASE; DISTRIBUTION IS UNLIMITED.

U.S. ARMY LABORATORY COMMAND

BALLISTIC RESEARCH LABORATORY  
ABERDEEN PROVING GROUND, MARYLAND

92-12918



92 5 14 036 1

## **NOTICES**

**Destroy this report when it is no longer needed. DO NOT return it to the originator.**

**Additional copies of this report may be obtained from the National Technical Information Service, U.S. Department of Commerce, 5285 Port Royal Road, Springfield, VA 22161.**

**The findings of this report are not to be construed as an official Department of the Army position, unless so designated by other authorized documents.**

**The use of trade names or manufacturers' names in this report does not constitute indorsement of any commercial product.**

REPORT DOCUMENTATION PAGE			Form Approved OMB No. 0704-0188	
Public reporting burden for this collection of information is estimated to average 1 hour per response, including the time for reviewing instructions, searching existing data sources, gathering and maintaining the data needed, and completing and reviewing the collection of information. Send comments regarding this burden estimate or any other aspect of this collection of information, including suggestions for reducing this burden, to Washington Headquarters Services, Directorate for Information Operations and Reports, 1215 Jefferson Davis Highway, Suite 1204, Arlington, VA 22202-4302, and to the Office of Management and Budget, Paperwork Reduction Project (0704-0188), Washington, DC 20503.				
1. AGENCY USE ONLY (Leave blank)		2. REPORT DATE May 1992		3. REPORT TYPE AND DATES COVERED Final Mar 91 - Aug 91
4. TITLE AND SUBTITLE The Effect of Yaw Cards on the Pitching and Yawing Motion of Symmetric Projectiles			5. FUNDING NUMBERS  1L162618AH80	
6. AUTHOR(S) Robert L. McCoy				
7. PERFORMING ORGANIZATION NAME(S) AND ADDRESS(ES)			8. PERFORMING ORGANIZATION REPORT NUMBER	
9. SPONSORING / MONITORING AGENCY NAME(S) AND ADDRESS(ES) USA Ballistic Research Laboratory ATTN: SLCBR-DD-T Aberdeen Proving Ground, MD 21005-5066			10. SPONSORING / MONITORING AGENCY REPORT NUMBER  BRL-TR-3338	
11. SUPPLEMENTARY NOTES				
12a. DISTRIBUTION / AVAILABILITY STATEMENT Approved for Public Release - Distribution is Unlimited			12b. DISTRIBUTION CODE	
13. ABSTRACT (Maximum 200 words)  This report presents an improved method for analysis of the effect of yaw cards on the determination of the pitching moment coefficient of symmetric missiles. Several comparisons of the present method are made with spark photography range results obtained for the same projectiles, and a proper treatment of yaw-card data is shown to significantly improve the agreement between the two techniques.				
14. SUBJECT TERMS Yaw Cards Pitching Motion Yawing Motion		Card Normal Force Pitch (motion) Card Overturning Moment Yaw Gyroscopic Stability		15. NUMBER OF PAGES 51
				16. PRICE CODE
17. SECURITY CLASSIFICATION OF REPORT UNCLASSIFIED	18. SECURITY CLASSIFICATION OF THIS PAGE UNCLASSIFIED	19. SECURITY CLASSIFICATION OF ABSTRACT UNCLASSIFIED	20. LIMITATION OF ABSTRACT SAR	

INTENTIONALLY LEFT BLANK.

# TABLE OF CONTENTS

	<u>Page</u>
LIST OF FIGURES . . . . .	v
LIST OF TABLES . . . . .	v
ACKNOWLEDGMENTS . . . . .	vii
1. INTRODUCTION . . . . .	1
2. YAW CARD FORCES AND MOMENTS . . . . .	2
3. THE DIFFERENTIAL EQUATION OF MOTION FOR A PROJECTILE FIRED THROUGH YAW CARDS . . . . .	3
4. SOLUTION OF THE DIFFERENTIAL EQUATION . . . . .	6
5. MEASUREMENT OF THE CARD OVERTURNING MOMENT . . . . .	8
6. THE EFFECT OF UNEQUALLY SPACED YAW CARDS . . . . .	9
7. EXPERIMENTAL RESULTS . . . . .	10
8. THE EFFECT OF YAW CARDS ON STABILITY . . . . .	13
9. CONCLUSIONS . . . . .	15
10. RECOMMENDATIONS . . . . .	15
11. REFERENCES . . . . .	31
LIST OF SYMBOLS . . . . .	33
DISTRIBUTION LIST . . . . .	37



<b>Accession For</b>	
NTIS GRA&I	<input checked="checked" type="checkbox"/>
DTIC TAB	<input type="checkbox"/>
Unannounced	<input type="checkbox"/>
Justification	
By _____	
Distribution/	
Availability Codes	
Dist	Avail and/or Special
A-1	

INTENTIONALLY LEFT BLANK.

## LIST OF FIGURES

<u>Figure</u>	<u>Page</u>
1 Train of Rectangular Waveform Pulses . . . . .	4
2 Sketch of the Caliber .30 Ball M1 Projectile . . . . .	17
3 Sketch of the Caliber .50 API M8 Projectile . . . . .	18
4 Sketch of the 20mm T215E1 Projectile . . . . .	19
5 Sketch of the 90MM M71 Shell . . . . .	20
6 Zero-Yaw Pitching Moment Coefficient versus Effective Card Density, Caliber .30 Ball M1 Projectile . . . . .	21
7 Zero-Yaw Pitching Moment Coefficient versus Effective Card Density, Caliber .50 API M8 Projectile . . . . .	22
8 Zero-Yaw Pitching Moment Coefficient versus Effective Card Density, 20mm T215E1 Projectile . . . . .	23
9 Zero-Yaw Pitching Moment Coefficient versus Effective Card Density, 90mm M71 Shell . . . . .	24

## LIST OF TABLES

<u>Table</u>	<u>Page</u>
1 Average Physical Characteristics of the Test Projectiles . . . . .	25
2 Yaw-Card Data for the Caliber .30 Ball M1 Projectile . . . . .	26
3 Yaw-Card Data for the Caliber .50 API M8 Projectile . . . . .	27
4 Yaw-Card Data for the 20MM T215E1 Projectile . . . . .	28
5 Yaw-Card Data for the 90MM M71 Shell . . . . .	29
6 Comparison of Yaw-Card and Spark Range Results . . . . .	30
7 Standard Deviations in $C_{M\alpha}$ . . . . .	30

INTENTIONALLY LEFT BLANK.



## ACKNOWLEDGMENTS

The author is indebted to Mr. J. Bradley of the Free Flight Aerodynamics Branch and to Dr. P. Plostins of the Fluid Physics Branch for their invaluable comments and suggestions, and to Ms. B. Willick of the Firing Tables Branch for her painstaking typing of the many equations of this report in the Latex word processor.

INTENTIONALLY LEFT BLANK.

## 1. INTRODUCTION

The use of yaw cards to determine the pitching and yawing motion of projectiles dates from the beginning of the twentieth century, with F. W. Mann's investigation of the flight of rifle bullets (Mann 1909). An excellent illustration of the method was provided by Fowler et al. (1920, 1922). Fowler noted that the presence of yaw cards affected the yawing motion, and attempted to correct the results for the card effect.

H. P. Hitchcock (1932) described the yaw-card test technique used at Aberdeen Proving Ground, Maryland, from about 1925 to 1950. During this period Hitchcock conducted numerous yaw-card firings of various projectiles, ranging in size from small arms bullets up to large caliber cannon artillery shell. Hitchcock's method for card-effect corrections (Hitchcock 1932, 1942) depended on firing through both dense and sparse distributions of cards, and using an empirical technique to correct the observed yaw period for the effect of the cards.

B. G. Karpov (1953) compared the results obtained from yaw cards for the 20mm T215E1 projectile (Hitchcock 1953) with those obtained in the Ballistic Research Laboratory (BRL) Free Flight Aerodynamics Range (Braun 1958). Karpov concluded that yaw-card test results are accurate to within ten percent for the pitching moment coefficient ( $C_{M\alpha}$ ), but are reliable only to the correct order of magnitude for the Magnus moment and pitch damping moment coefficients. Karpov reiterated Hitchcock's empirical correction for the card effect, but did not attempt an independent analysis.

The spark photography range (Braun 1958; Rogers 1958; Kittyle et al. 1987) has generally replaced the yaw-card range for modern aeroballistic testing. The principal advantages of spark photography over yaw cards are an order of magnitude higher precision of measurement, no interference with the free flight of the projectile, and high quality flowfield visualization provided by the spark shadowgraphs. In spite of these advantages, however, yaw cards are still used, often because of the high cost of spark range testing, and sometimes because test projectiles involve either discarding parts that are hazardous to expensive instrumentation, or toxic materials that cannot be fired in spark ranges due to environmental restrictions.

This report presents an improved method for analysis of the effect of yaw cards on the determination of the pitching moment coefficient. Several comparisons of the present method are made with spark range results obtained for the same projectiles, and a proper treatment of yaw-card data is shown to significantly improve the agreement between the two experimental techniques.

## 2. YAW CARD FORCES AND MOMENTS

The forces and moments experienced by a projectile as it perforates a yaw card are fundamentally impulsive in nature. The projectile punches a hole in the card material; for small yaw, the hole is nearly circular in shape and is approximately the diameter of the projectile. The card forces and moments are assumed to depend on several variables, including the projectile reference diameter, the density of the yaw card material, the card thickness, the striking velocity, and the angle of attack at card impact. Application of the theory of dimensional analysis (Hunsaker and Rightmire 1947) to the impact of the projectile with a yaw card leads to the following specification of the card drag force, the card normal force and the card overturning moment:

$$F_{D_c} = \frac{\pi}{4} \rho_c d \tau_c V^2 C_{D_c}, \quad (1)$$

$$F_{N_c} = \frac{\pi}{4} \rho_c d \tau_c V^2 C_{N_{\alpha_c}} \sin \alpha_t, \quad (2)$$

$$M_{M_c} = \frac{\pi}{4} \rho_c d^2 \tau_c V^2 C_{M_{\alpha_c}} \sin \alpha_t, \quad (3)$$

where:

$F_{D_c}$  = card drag force

$F_{N_c}$  = card normal force

$M_{M_c}$  = card overturning moment

$C_{D_c}$  = card drag coefficient

$C_{N_{\alpha_c}}$  = card normal force coefficient

$C_{M_{\alpha_c}}$  = card overturning moment coefficient

$\rho_c$  = density of the card material

$d$  = projectile reference diameter

$\tau_c$  = card thickness

$V$  = speed of projectile at card at impact

$\alpha_t = (\alpha^2 + \beta^2)^{\frac{1}{2}}$ , total angle of attack

$\alpha$  = angle of attack

$\beta$  = angle of sideslip.

To the author's knowledge, no experimental measurements of card drag or card normal forces have been made. However, in Section 7 of this report, the present theory for the card overturning moment is shown to accurately predict the results of several yaw card experiments; this fact provides some justification for the assumptions made above regarding the nature of yaw card forces and moments.

The effect of the card overturning moment on the pitching and yawing motion of a symmetric projectile will now be considered.

### 3. THE DIFFERENTIAL EQUATION OF MOTION FOR A PROJECTILE FIRED THROUGH YAW CARDS

C. H. Murphy (1963) has derived the differential equation of pitching and yawing motion for a spinning, symmetric projectile, acted on by a linear pitching moment:

$$\ddot{\xi} - i P \dot{\xi} - M \xi = 0, \quad (4)$$

where:

$$\xi \approx \sin \beta + i \sin \alpha, \text{ the complex yaw}$$

$$P = \left( \frac{I_x}{I_y} \right) \left( \frac{p d}{V} \right)$$

$$M = \frac{\rho S d^3}{2 I_y} C_{M\alpha}$$

$$I_x = \text{axial moment of inertia}$$

$$I_y = \text{transverse moment of inertia}$$

$$p = \text{axial spin}$$

$$\rho = \text{air density}$$

$$S = \pi d^2 / 4, \text{ reference area}$$

$$C_{M\alpha} = \text{aerodynamic pitching moment coefficient.}$$

If the card overturning moment,  $M_{M_c}$ , from equation (3) is included in Murphy's derivation, it is found that the coefficient of  $\xi$  in equation (4) should be replaced by  $- [M + M_c I(s)]$ , where  $I(s)$  is a function whose value is unity at each yaw-card location, and zero elsewhere. The term  $M_c$  is:

$$M_c = \frac{\pi \rho_c \tau_c d^4}{4 I_y} C_{M_{\alpha c}}. \quad (5)$$

The function  $I(s)$  is readily obtained for uniformly spaced yaw cards, by means of a Fourier series. (The effect of non-uniformly spaced cards will be discussed later.)

Consider a train of rectangular waveform pulses, spaced at equal intervals along the  $s$ -axis, where  $s$  is distance in calibers. Figure 1 illustrates this pulse function.

The pulses are spaced at equal intervals,  $S_c$ , and each pulse acts over an arbitrary interaction distance,  $l$ , in calibers. The height of each pulse is  $1/l$ , so that the area under each pulse is unity:

$$\int_{n S_c - l/2}^{n S_c + l/2} I(s) ds = 1, \quad (6)$$

$$\text{i.e., } I(s) = 1/l, \text{ for } (n S_c - l/2) < s < (n S_c + l/2), \quad (7)$$

$$\text{and } I(s) = 0, \text{ otherwise.} \quad (8)$$

The pulse function  $I(s)$  is often called the "filter function", because the product of  $I(s)$  and any other function leaves the other function unchanged wherever the pulse occurs, and reduces it identically to zero elsewhere.

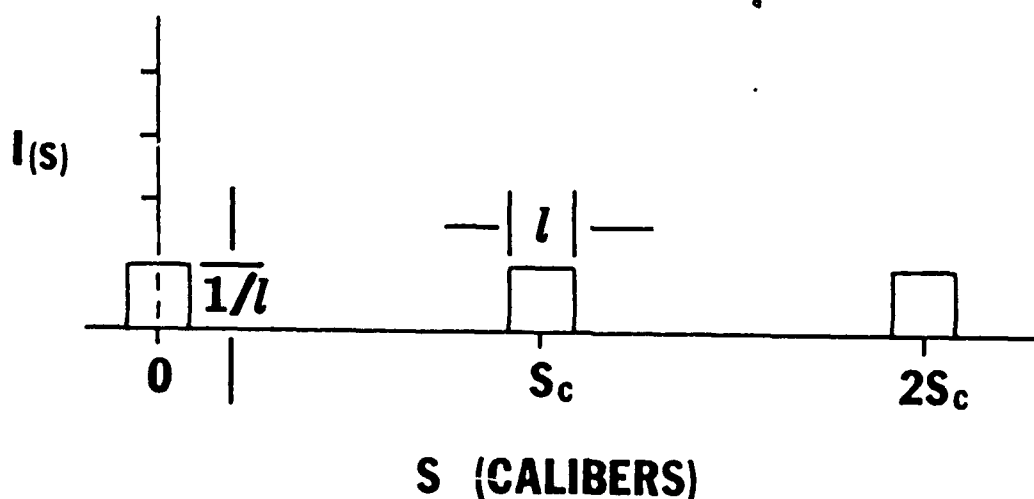


Figure 1. Train of Rectangular Waveform Pulses.

The Fourier series expansion (Wylie 1960) of the even function  $I(s)$  is:

$$I(s) = \frac{1}{2} a_0 + \sum_{n=1}^{\infty} a_n \cos \left( \frac{2 \pi n s}{S_c} \right), \quad (9)$$

where:

$$a_0 = \frac{2}{S_c} \int_0^{S_c} I(s) ds \quad (10)$$

$$a_n = \frac{2}{S_c} \int_0^{S_c} I(s) \cos \left( \frac{2 \pi n s}{S_c} \right) ds. \quad (11)$$

Performing the indicated integrations:

$$a_0 = \frac{2}{S_c} \quad (12)$$

$$a_n = \frac{2}{\pi n l} \sin \left( \frac{\pi n l}{S_c} \right). \quad (13)$$

Substituting equations (12) and (13) into equation (9):

$$I(s) = \frac{1}{S_c} + \frac{2}{\pi l} \sum_{n=1}^{\infty} \frac{1}{n} \sin \left( \frac{\pi n l}{S_c} \right) \cos \left( \frac{2 \pi n s}{S_c} \right). \quad (14)$$

For equally spaced yaw cards, the product of the function  $I(s)$  and the card moment  $M_c$  correctly represents the effect of the card overturning moment on the flight of the projectile. If this product is added to  $M$  in equation (4):

$$\tilde{\xi}'' - i P \tilde{\xi}' - \left[ M + \frac{M_c}{S_c} + \frac{2 M_c}{\pi l} \sum_{n=1}^{\infty} \frac{1}{n} \sin \left( \frac{\pi n l}{S_c} \right) \cos \left( \frac{2 \pi n s}{S_c} \right) \right] \tilde{\xi} = 0. \quad (15)$$

Equation (15) is the differential equation of pitching and yawing motion for a symmetric projectile acted on by a linear pitching moment, and fired through a series of uniformly spaced yaw cards.

#### 4. SOLUTION OF THE DIFFERENTIAL EQUATION

If the card overturning moment were zero, the solution to equation (15) would be (Murphy 1963):

$$\tilde{\xi} = K_1 e^{i\phi_1} + K_2 e^{i\phi_2}, \quad (16)$$

where  $\phi_j = \phi_{j0} + \phi'_j s$ , for  $j = 1, 2$ .

Equation (16) is also known to accurately describe the observed pitching and yawing motions of spinning projectiles fired on yaw-card ranges (Fowler et al. 1920; Hitchcock 1932). Thus it is natural to try equation (16) as a solution of equation (15). Differentiating equation (16) gives:

$$\tilde{\xi}' = i\phi'_1 K_1 e^{i\phi_1} + i\phi'_2 K_2 e^{i\phi_2} \quad (17)$$

$$\tilde{\xi}'' = -\phi_1'^2 K_1 e^{i\phi_1} - \phi_2'^2 K_2 e^{i\phi_2}. \quad (18)$$

Equations (16), (17), and (18) are now substituted into equation (15):

$$\begin{aligned} & K_1 e^{i\phi_1} \left[ -\phi_1'^2 + P\phi_1' - \left( M + \frac{M_c}{S_c} \right) \right] + K_2 e^{i\phi_2} \left[ -\phi_2'^2 + P\phi_2' - \left( M + \frac{M_c}{S_c} \right) \right] \\ &= \frac{2M_c}{\pi l} \left[ K_1 e^{i\phi_1} + K_2 e^{i\phi_2} \right] \sum_{n=1}^{\infty} \frac{1}{n} \sin \left( \frac{\pi n l}{S_c} \right) \cos \left( \frac{2\pi n s}{S_c} \right). \end{aligned} \quad (19)$$

Dividing equation (19) by  $K_1 e^{i\phi_1}$  and transposing terms:

$$\begin{aligned} -\phi_1'^2 + P\phi_1' - \left( M + \frac{M_c}{S_c} \right) &= - \left[ -\phi_2'^2 + P\phi_2' - \left( M + \frac{M_c}{S_c} \right) \right] K_2 K_1^{-1} e^{-i\hat{\phi}} \\ &+ \frac{2M_c}{\pi l} \left[ 1 + \frac{K_2}{K_1} e^{-i\hat{\phi}} \right] \sum_{n=1}^{\infty} \frac{1}{n} \sin \left( \frac{\pi n l}{S_c} \right) \cos \left( \frac{2\pi n s}{S_c} \right) \end{aligned} \quad (20)$$

where  $\hat{\phi} = \phi_1 - \phi_2$ .



Following Murphy's argument (Murphy 1963), the first term on the right-hand side of equation (20) is a small periodic term that has no significant effect on the constant terms of the left-hand side. The last term on the right-hand side of equation (20) is a convergent infinite series of fluctuating terms, and its influence is obtained by computing its average over an arbitrary number of equally spaced yaw cards.

$$\text{Let } T_n = \frac{1}{n} e^{-i\psi} \sin\left(\frac{\pi n l}{S_c}\right) \cos\left(\frac{2\pi n s}{S_c}\right), \quad (21)$$

where:

$$n = 1, 2, 3, \dots$$

$$\psi = \hat{\phi} \text{ or } 0$$

$$T_n = \text{any term in the infinite series.}$$

If  $N_c$  is the total number of yaw cards, equally spaced a distance  $S_c$  calibers apart, the average value of  $T_n$  over the distance  $N_c S_c$  is:

$$[T_n]_{AV} = \frac{1}{N_c S_c} \int_0^{N_c S_c} \frac{1}{n} e^{-i\psi} \sin\left(\frac{\pi n l}{S_c}\right) \cos\left(\frac{2\pi n s}{S_c}\right) ds. \quad (22)$$

The integral in equation (22) is obtained from a table of integrals, found in standard mathematical handbooks:

$$\begin{aligned} [T_n]_{AV} = \frac{2\pi e^{-i\psi} \sin(\pi n l / S_c)}{N_c S_c [(2\pi n)^2 - (\psi' S_c)^2]} \{ \sin(2\pi n N_c) \\ - i\psi' \left(\frac{S_c}{2\pi n}\right) [\cos(2\pi n N_c) - 1] \}. \end{aligned} \quad (23)$$

Both  $n$  and  $N_c$  are integers, and the numerator of equation (23) is therefore identically zero, for all values of  $n$  and  $N_c$ . The denominator can be zero only for resonance, i.e., for one yaw card per period of the yawing motion. However, at least three yaw cards per period must be used to obtain a satisfactory yaw reduction, and in practice, the denominator of equation (23) will never be zero.

The average value of every term in the infinite series of equation (20) is therefore zero, over any arbitrary number of equally spaced yaw cards. Equation (20) may now be averaged with the aid of this result, and solved for  $\phi'_1$ :

$$\phi'_1 = \frac{1}{2} \left[ P + \sqrt{P^2 - 4 (M + M_c / S_c)} \right]. \quad (24)$$

A similar result is obtained for the other mode, and its frequency is:

$$\phi'_2 = \frac{1}{2} \left[ P - \sqrt{P^2 - 4 (M + M_c / S_c)} \right]. \quad (25)$$

Equation (16), together with equations (24) and (25), is therefore the approximate general solution of equation (15).

## 5. MEASUREMENT OF THE CARD OVERTURNING MOMENT

Data reduction for either spark ranges or yaw-card ranges consists of fitting equation (16) to the observed pitching and yawing motion of the projectile. The observed, or "range" values of the two epicyclic frequencies are then used to determine the range value of the pitching moment acting on the projectile. For yaw-card firings through uniformly spaced cards, the product of equations (24) and (25) is:

$$\phi'_{1(R)} \cdot \phi'_{2(R)} = M_{(R)} = M + \frac{M_c}{S_c} \quad (26)$$

where the (R)-subscript indicates the observed, or "range" value.

The range value of the pitching moment coefficient is:

$$C_{M_{\alpha(R)}} = \frac{8 I_y}{\pi \rho d^5} \phi'_{1(R)} \cdot \phi'_{2(R)} = \frac{8 I_y}{\pi \rho d^5} \left( M + \frac{M_c}{S_c} \right). \quad (27)$$

From equations (4) and (5):

$$M = \frac{\pi \rho d^5}{8 I_y} C_{M_\alpha} \quad (28)$$

$$\frac{M_c}{S_c} = \frac{\pi \rho_c \tau_c d^4}{4 I_y S_c} C_{M_{\alpha c}} \quad (29)$$

Substitution of equations (28) and (29) into equation (27) yields:

$$C_{M_{\alpha(R)}} = C_{M_\alpha} + C_{M_{\alpha c}} \tilde{D}_c, \quad (30)$$

$$\text{where } \tilde{D}_c = \left[ \left( \frac{\rho_c}{\rho} \right) \left( \frac{\tau_c}{d} \right) \left( \frac{2}{S_c} \right) \right], \text{ the effective card density.} \quad (31)$$

Equation (30) shows that if range values of the pitching moment coefficient from yaw-card firings are plotted against the effective card density,  $\tilde{D}_c$ , the data should fall along a straight line whose intercept is the aerodynamic pitching moment coefficient,  $C_{M_\alpha}$ , and whose slope is the card overturning moment coefficient,  $C_{M_{\alpha c}}$ .

The effective card density,  $\tilde{D}_c$ , is the dimensionless triple product of the ratio of card material density to air density, the card thickness in calibers, and twice the reciprocal of the card spacing. Equation (31) illustrates the fact that dense or sparse card distributions can be readily obtained by varying either the card thickness or the card spacing, or a combination of both.

## 6. THE EFFECT OF UNEQUALLY SPACED YAW CARDS

For uniform card spacing, equations (24) and (25) show that the epicyclic frequencies are constant, for any spinning or non-spinning symmetric projectile acted on by a linear pitching moment and a linear card overturning moment. If the card spacing varies over the length of the firing range, the epicyclic frequencies also vary along the trajectory.

For an arbitrarily irregular card spacing, no analytical solution of the problem appears feasible, and numerical methods would have to be employed. Fortunately, most yaw-card

firings are done with at least piecewise regular card spacing; various sections of the firing range are often instrumented with different card spacings, but the spacing within a given section remains constant. For piecewise regular card spacing, the approximate analytical solution of the differential equation is everywhere valid, but the observed epicyclic frequencies reflect average values over the total length of the instrumented firing range.

A modern yaw-card firing deserves modern data reduction procedures. The epicyclic solution (Murphy 1963) should be fitted to the yaw-card data using nonlinear least squares, in lieu of graphical methods (Fowler et al. 1920; Hitchcock 1932). Variations in the epicyclic frequencies caused by irregular card spacing degrade the accuracy of the least squares fit, and a uniform card spacing should therefore be used over the entire instrumented length of the firing range.

## 7. EXPERIMENTAL RESULTS

Several opportunities currently exist for a direct comparison of yaw-card results with those obtained for the same projectiles in spark photography ranges. The 20mm T215E1 firings in the two facilities (Karpov 1953; Hitchcock 1953) were mentioned in the introduction. Recent spark photography range tests of the 7.62mm M118 Match bullet (McCoy 1988) and the caliber .50 API M8 bullet (McCoy 1990) provide further comparisons. The 7.62mm M118 is a match-grade version of the caliber .30 Ball M1 projectile (Hitchcock 1942) fired through yaw cards in 1939. H. P. Hitchcock fired the caliber .50 API M8 bullet (Hitchcock 1943) through yaw cards on the Aberdeen Proving Ground small arms range in 1943.

A limited search for a large caliber shell comparison provided a fourth example. H. P. Hitchcock fired the 90mm T8 shell (later type-classified as the M71) through yaw cards (Hitchcock 1941) and E. D. Boyer reported the results of 90mm M71 firings in the BRL Transonic Range (Boyer 1963). The T8 shell were fitted with the M43 fuze, and the Transonic Range firings of the M71 shell used the M73 fuze. The two fuzes have similar exterior contours, and virtually identical weights.

Physical characteristics of the test projectiles were independently determined for the various yaw-card firings and the spark photography range tests. Table 1 lists the average physical characteristics used in the yaw card and the spark range data reductions, for the four illustrative examples of this report. Sketches of the four projectiles are shown in Figures 2 through 5.

In addition to the physical characteristics, H. P. Hitchcock measured the air temperature, air density, instrumental velocity, the average observed yaw period over several cycles of the motion, and the average rate of change of the yaw orientation angle, for each round fired through yaw cards. (Hitchcock referred to the rate of change of yaw orientation as "linear rate of precession.") The relationships between Hitchcock's yaw period and linear precession rate, and the two characteristic epicyclic frequencies are (Hitchcock 1942; Murphy 1963):

$$\phi'_1 + \phi'_2 = 2 \pi d (\phi' / \pi), \quad (32)$$

$$\phi'_1 - \phi'_2 = \frac{2 \pi d}{L}, \quad (33)$$

where:

$\phi'_1$  = fast arm frequency (radians/calibers)

$\phi'_2$  = slow arm frequency (radians/calibers)

$d$  = projectile reference diameter (feet)

$L$  = average yaw period (feet)

$(\phi' / \pi)$  = linear rate of precession (semi-revolution/foot).

Range values of the epicyclic frequencies are readily obtained from the yaw-card data, with the help of equations (32) and (33), and range values of the pitching moment coefficient are determined by means of equation (27). The Mach number corresponding to each value of  $C_{M_{\alpha(R)}}$  is obtained from the instrumental velocity and the atmospheric properties at time of firing.

The methodology used by Hitchcock (1932, 1942) did not anticipate the existence of nonlinear pitching moments, although a dependence of aerodynamic drag on yaw level was

generally understood. The four projectiles considered in this report are known to have nonlinear pitching moments, from the spark range data analysis. Murphy (1963) has shown that a cubic pitching moment results in a dependence of the range values of  $C_{M_\alpha}$  on the effective squared yaw:

$$C_{M_\alpha(R)} = C_{M_{\alpha 0}} + C_2 \delta_e^2, \quad (34)$$

$$\delta_e^2 = K_1^2 + K_2^2 + \frac{\phi'_1 K_1^2 - \phi'_2 K_2^2}{\phi'_1 - \phi'_2}, \quad (35)$$

where:

$C_{M_{\alpha 0}}$  = zero-yaw pitching moment coefficient

$C_2$  = cubic pitching moment coefficient

$\delta_e^2$  = effective squared yaw.

From Hitchcock's measurements of the average maximum and minimum yaw, and the two epicyclic frequencies, an approximate value of  $\delta_e^2$  was obtained for each yaw-card data round.

The effective card density,  $\tilde{D}_c$ , was determined for each round, using an average card material density of 1041 kg/m<sup>3</sup> (65 lb/ft<sup>3</sup>) for photographic paper yaw cards, and 577 kg/m<sup>3</sup> (36 lb/ft<sup>3</sup>) for the cardboard commonly used at Aberdeen Proving Ground for large caliber firings. The average card thickness is 0.165 mm (0.0065 inch) for photographic paper, and 1.59 mm (1/16 inch) for standard cardboard. H. P. Hitchcock used piecewise regular card spacing for all the yaw-card firings considered in this report, and an average card spacing for each round was determined.

The range values of  $C_{M_\alpha}$  from the yaw-card firings were corrected to a central Mach number for each projectile, using a local slope ( $\partial C_{M_\alpha} / \partial M_\infty$ ) obtained from analysis of the spark range data. In most cases this correction is small, but it allows a direct comparison of results to be made, without contamination due to Mach number effects. The round-by-round yaw-card data are listed in Tables 2 through 5, for the four example projectiles.

If a symmetric projectile acted on by a cubic pitching moment is fired on a yaw-card range, the range values of the pitching moment coefficient vary with both the effective squared yaw and the effective card density:

$$C_{M_\alpha(R)} = C_{M_{\alpha 0}} + C_2 \delta_e^2 + C_{M_{\alpha c}} \tilde{D}_c. \quad (36)$$

The analysis of yaw-card pitching moment data thus requires multiple linear regression least squares. The results of fitting equation (36) to the data of Tables 2 through 5 is shown in Table 6, which compares the values of  $C_{M_{\alpha 0}}$  and  $C_2$  obtained from the yaw-card firings with the spark range results for the same projectiles. The comparisons are very encouraging.

The difference between the spark range and yaw-card values of  $C_{M_{\alpha 0}}$  is everywhere less than 2 percent, and the cubic coefficients obtained by the two methods are in fairly good agreement. The yaw-card value of  $C_2$  obtained for the caliber .30 Ball M1 bullet was poorly determined, and no cubic coefficient could be found from spark range tests of the 20mm T215E1, because the spark range rounds were all fired at small yaw levels.

The last column in Tables 2 through 5 lists the round-by-round yaw-card values of  $C_{M_{\alpha 0}}$ , obtained by means of the cubic pitching moment coefficients and the effective squared yaws. Figures 6 through 9 illustrate the variation of  $C_{M_{\alpha 0}}$  with effective card density for the four example projectiles. The slopes of the least squares lines in Figures 6 through 9 are the card overturning moment coefficients listed in Table 6. Note that for typical dense distributions of yaw cards, the intercepts are more than 20 percent below the uncorrected values. The solid circles on the four plots are the average values of  $C_{M_{\alpha 0}}$  obtained from analysis of the spark range data.

A final comparison of the round-to-round data scatter between the two methods is illuminating. The standard deviation of the least squares fit of equation (36) to the yaw-card data is compared with the standard deviation in  $C_{M_{\alpha 0}}$  obtained from analysis of the spark range data. The results are listed in Table 7.

The standard deviation in  $C_{M_{\alpha 0}}$  obtained from yaw-card data averages about 3 times that observed from the spark range firings. This difference reflects the effect of lower measurement precision for yaw-card firings. However, the yaw-card standard deviations average less than 4 percent of  $C_{M_{\alpha 0}}$ , which is sufficiently good for nearly all practical purposes.

## 8. THE EFFECT OF YAW CARDS ON STABILITY

The gyroscopic stability criterion for a symmetric projectile is derived in Murphy (1963):

$$P^2 - 4 M > 0. \quad (37)$$

For statically stable missiles,  $M' < 0$ , and equation (37) shows that a statically stable missile is always gyroscopically stable, regardless of spin. If the projectile is statically unstable ( $M > 0$ ), equation (37) states the amount of axial spin required to achieve gyroscopic stability:

$$P^2 > 4 M. \quad (38)$$

For many years, exterior ballisticians have used the gyroscopic stability factor:

$$S_g = P^2 / 4 M. \quad (39)$$

Equations (38) and (39) combine to give the classical definition of the gyroscopic stability criterion for statically unstable, spin-stabilized projectiles:

$$S_g = P^2 / 4 M > 1. \quad (40)$$

If the projectile is fired through yaw cards, the term  $M$  in equations (37) through (39) is replaced by  $(M + M_c / S_c)$ , and the two gyroscopic stability criteria become:

$$S_g = \frac{P^2}{4 (M + M_c / S_c)} > 1, \quad (41)$$

for statically unstable projectiles, and:

$$(M + M_c / S_c) < 0, \quad (42)$$

for statically stable missiles.

Table 6 shows that both  $M$  and  $M_c$  are positive for typical spin-stabilized projectiles, and equation (41) thus contains the warning that a sufficiently dense distribution of yaw cards could cause a marginally stable shell to become gyroscopically unstable! For cases involving suspected marginal stability, one recourse available to the program engineer is to conduct the yaw-card firings with a gun having a faster twist of rifling, then convert the gyroscopic stability measurements to the desired spin rate.

The effect of yaw cards on the behavior of statically stable missiles is uncertain, as no systematic tests have been conducted. Modern finned missiles have relatively sharp fin leading edges, which cut the yaw cards without punching out a significant amount of the card



material. The effective "center of pressure" of the card normal force is probably forward of the center of gravity for missiles with sharp leading edge fins, and the card moment may well be destabilizing for finned missiles. Equation (42) shows that for  $M < 0$  and  $M_c > 0$ , a very dense distribution of yaw cards could cause a finned missile to become statically unstable. If a flare-stabilized configuration is fired through yaw cards, and the flare tail punches out a large area of the card, the net card moment could well be negative. A limited experimental investigation of the card effect for finned and flare-stabilized projectiles is needed to resolve the matter.

## 9. CONCLUSIONS

An approximate analytical method has been presented, which properly accounts for the effect of yaw cards on the pitching and yawing motion of a symmetric projectile. The effect of card spacing is addressed, and the results show that uniform card spacing is always desirable.

Four example comparisons are made of the improved yaw-card method with spark photography range data for the same projectiles. The results show agreement to within 2 percent difference between the two techniques, for the zero-yaw pitching moment coefficient. The improved method is capable of differentiating between nonlinear aerodynamic effects and card moment effects, and fairly good agreement is observed between yaw-card and spark range determinations of the cubic pitching moment.

The effect of yaw cards on gyroscopic stability is presented. Very dense distributions of yaw cards are shown to be destabilizing for statically unstable, spin-stabilized projectiles. A similar destabilizing effect on statically stable finned missiles is shown to be possible, for very dense distributions of yaw cards. A limited yaw-card experiment with finned and flare-stabilized missiles is needed to determine the card effect for statically stable configurations.

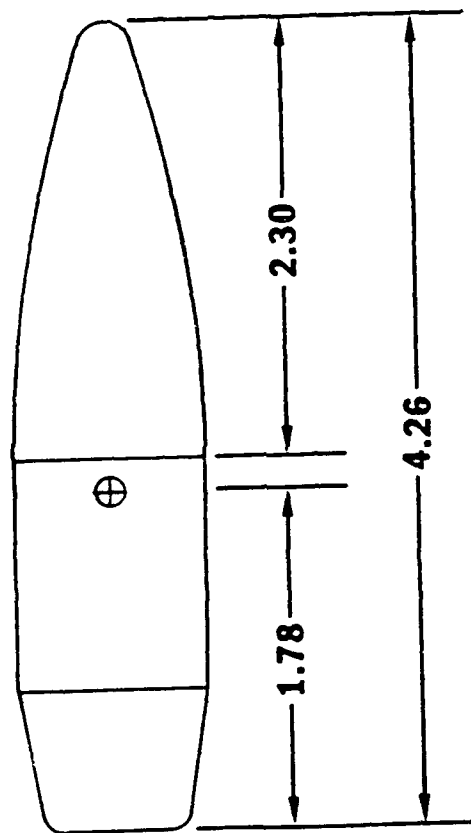
## 10. RECOMMENDATIONS

Uniform card spacing over the entire instrumented length of the firing range is recommended for all future yaw-card testing. Data rounds must be fired through both dense and sparse card distributions, to permit determination of the card overturning moment.

The effect of yaw cards is generally destabilizing, thus a minimum number of cards should always be used, consistent with requirements for good quality results. The data section length should cover at least one full cycle of the slower epicyclic yaw arm, and a minimum of three

data points per cycle of the fast arm should be used.

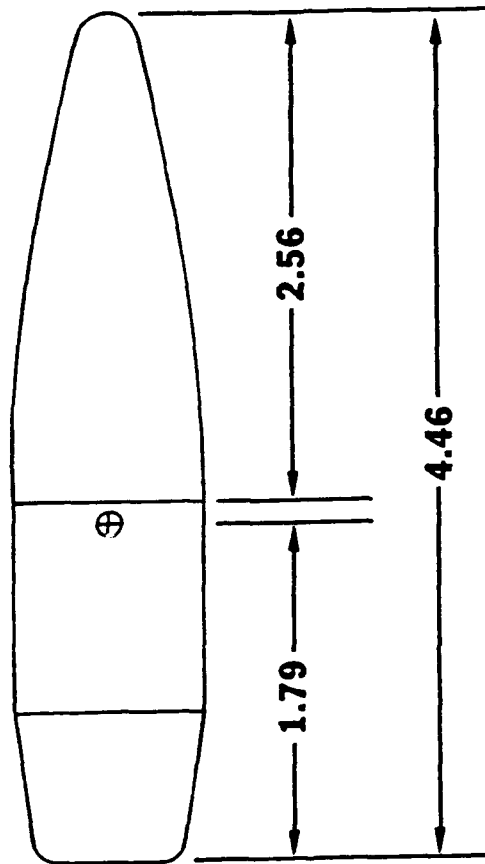
The card overturning moment for finned and flare-stabilized missiles has not been investigated. It is recommended that a limited experimental program be conducted for statically stable missiles, to determine the behavior of the card moment coefficient for such configurations.



**ALL DIMENSIONS IN CALIBERS**

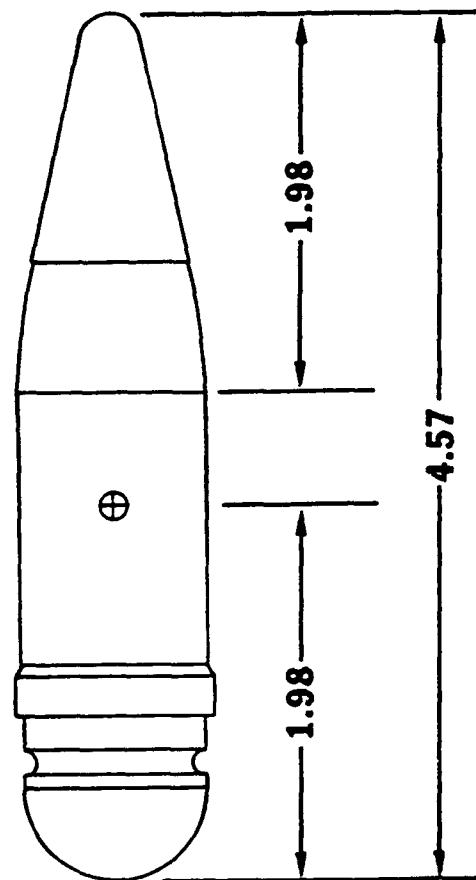
**(1 CALIBER 7.82mm)**

**Figure 2. Sketch of the Caliber .30 Ball M1 Projectile .**



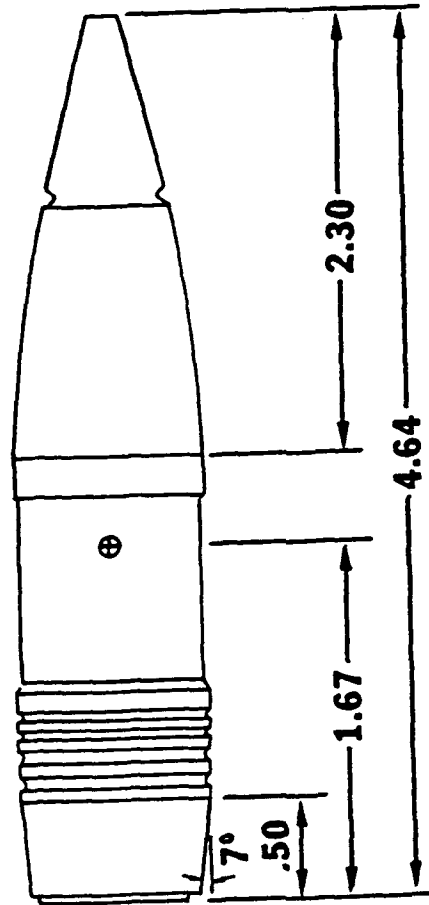
**ALL DIMENSIONS IN CALIBERS**  
**(1 CALIBER 12.95)**

**Figure 3. Sketch of the Caliber .50 API M8 Projectile .**



**ALL DIMENSIONS IN CALIBERS**  
**(1 CALIBER 19.89mm)**

**Figure 4. Sketch of the 20mm T215E1 Projectile.**



**ALL DIMENSIONS IN CALIBERS  
(1 CALIBER 89.26mm)**

**Figure 5. Sketch of the 90MM M71 Shell.**

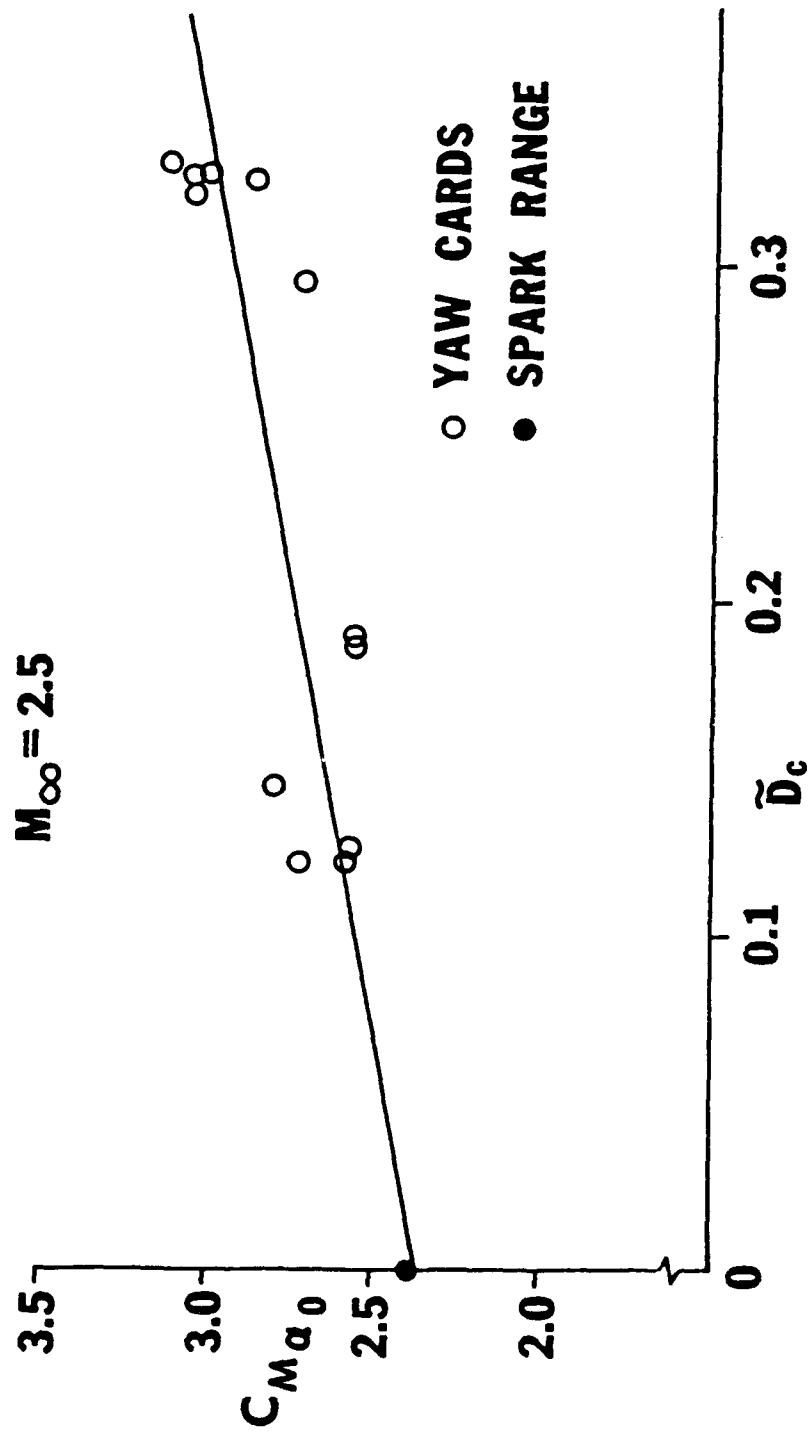


Figure 6. Zero-Yaw Pitching Moment Coefficient versus Effective Card Density,  
Caliber .30 Ball M1 Projectile.

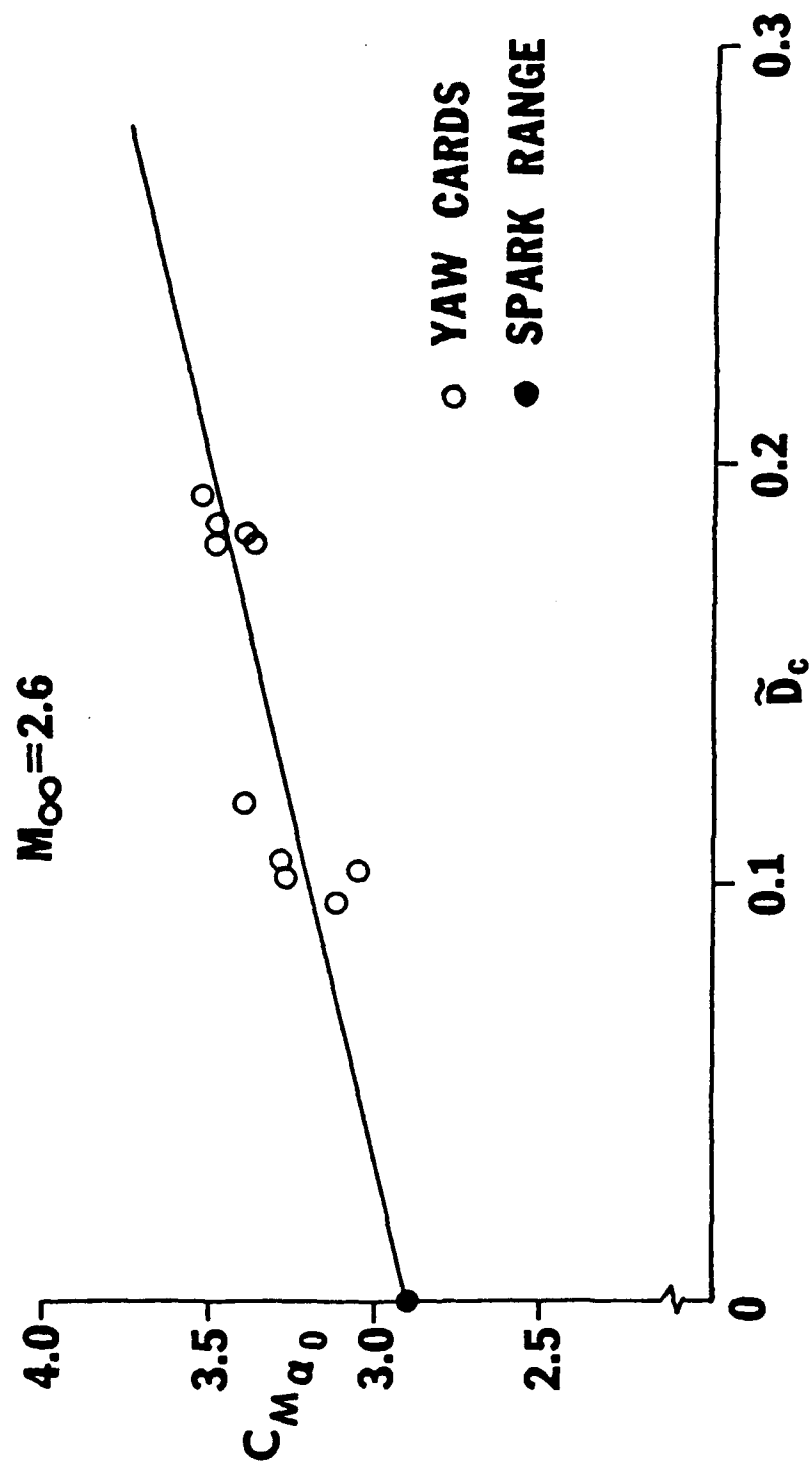


Figure 7. Zero-Yaw Pitching Moment Coefficient versus Effective Card Density,  
Caliber .50 API M8 Projectile.



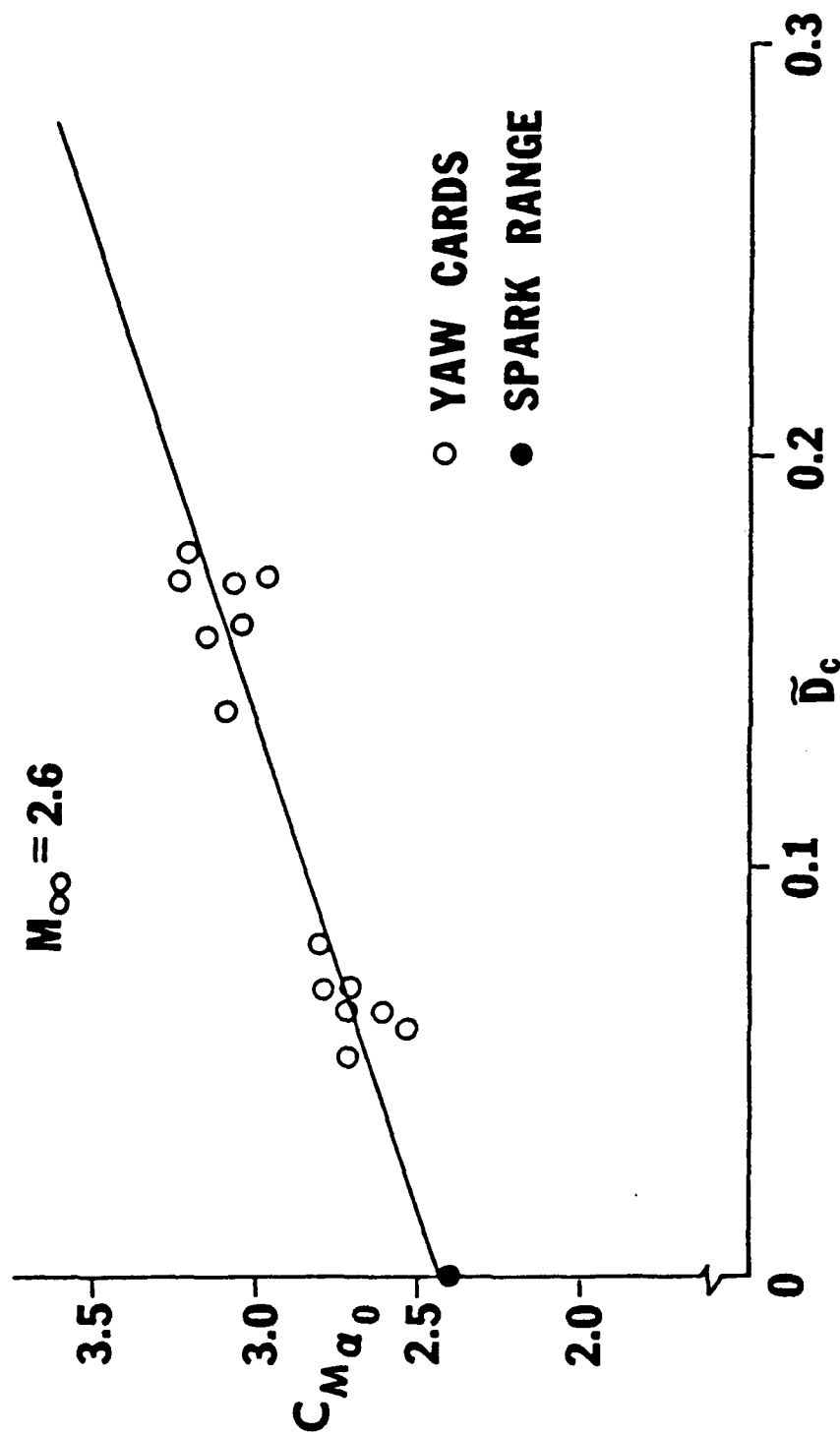


Figure 8. Zero-Yaw Pitching Moment Coefficient versus Effective Card Density, 20mm T215E1 Projectile.

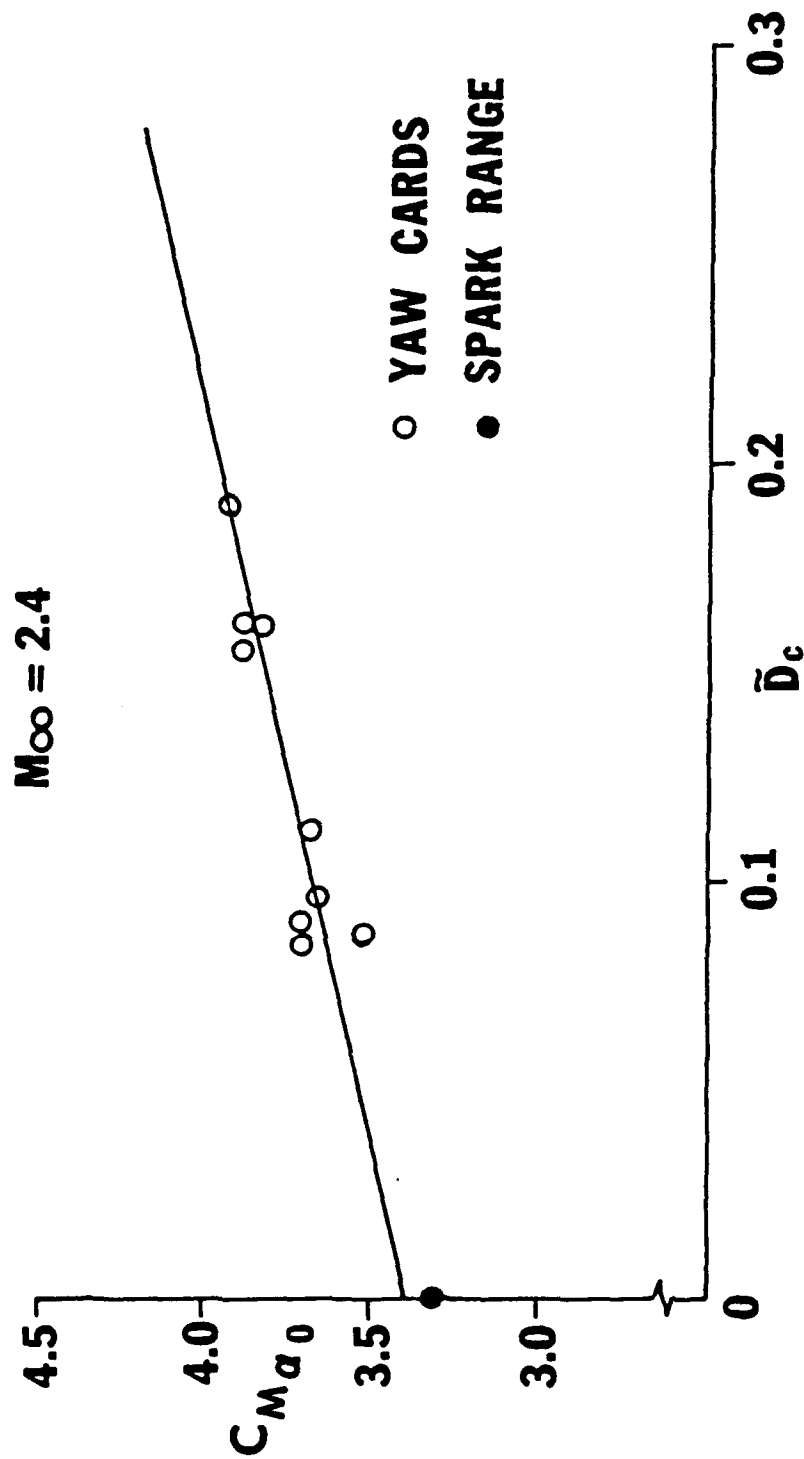


Figure 9. Zero-Yaw Pitching Moment Coefficient versus Effective Card Density,  
90mm M71 Shell.

Table 1. Average Physical Characteristics of the Test Projectiles.

Projectile	Reference Diameter	Total Length	Weight	Center of Gravity	Axial Moment of Inertia	Transverse Moment of Inertia
	(mm)	(calibers)	(grams)	(cal-base)	(gm-cm <sup>2</sup> )	(gm-cm <sup>2</sup> )
Cal. .30 Ball M1*	7.82	4.26	11.15	1.78	0.73	6.86
7.62MM M118**	7.82	4.19	11.27	1.79	0.72	6.78
Cal. .50 API M8*	12.95	4.49	42.3	1.79	7.90	75.0
Cal. .50 API M8**	12.95	4.46	42.0	1.79	7.84	73.9
20MM T215E1*	19.89	4.57	103.8	1.98	55.7	608
20MM T215E1**	19.89	4.57	104.2	1.98	56.1	610
90MM M71*	89.26	4.63	10.52(a)	1.75	0.0116(b)	0.110(b)
90MM M71**	89.26	4.64	10.62(a)	1.67	0.0117(b)	0.111(b)

\* Average values used in yaw-card data reduction

\*\* Average values used in Spark Range data reduction

(a) Weight in kilograms

(b) Moment of inertia in kilogram-meters<sup>2</sup>

Table 2. Yaw-Card Data for the Caliber .30 Ball M1 Projectile.

Round Number	Mach Number	$\phi'_1$ (rad/cal)	$\phi'_2$ (rad/cal)	$C_{M_\alpha}$	$\delta_e^2$	$\bar{D}_c$	$C_{M_\alpha}$ [ $M_\infty = 2.5$ ]*	$C_{M_{\alpha_0}}$ [ $M_\infty = 2.5$ ]**
8 (D)	2.39	.0157	.0040	2.96	.0509	.330	2.90	3.14
9 (D)	2.40	.0154	.0039	2.88	.0483	.332	2.83	3.06
10 (D)	2.38	.0155	.0038	2.83	.0634	.326	2.77	3.07
11 (S)	2.37	.0162	.0033	2.55	.0693	.144	2.48	2.81
12 (S)	2.40	.0163	.0032	2.48	.0335	.122	2.43	2.59
13 (S)	2.37	.0163	.0032	2.48	.0671	.122	2.41	2.73
14 (D)	2.54	.0162	.0031	2.42	.0641	.295	2.44	2.74
15 (D)	2.57	.0155	.0038	2.85	.0273	.327	2.89	3.02
17 (D)	2.51	.0159	.0035	2.65	.0470	.326	2.66	2.88
18 (S)	2.54	.0163	.0031	2.40	.0319	.187	2.42	2.57
19 (S)	2.51	.0163	.0030	2.37	.0403	.188	2.38	2.57
20 (S)	2.57	.0163	.0031	2.41	.0278	.125	2.45	2.58

All rounds were fired in December 1939 (Hitchcock 1942)

(D) Indicates dense distribution of cards

(S) Indicates sparse distribution of cards

\*  $C_{M_\alpha}$  corrected to  $M_\infty = 2.5$  using  $\frac{\partial C_{M_\alpha}}{\partial M_\infty} = -0.53$

\*\*  $C_{M_\alpha}$  corrected to zero yaw using  $C_2 = -4.7$

Table 3. Yaw-Card Data for the Caliber .50 API M8 Projectile.

Round Number	Mach Number	$\phi'_1$ (rad/cal)	$\phi'_2$ (rad/cal)	$C_{M_\alpha}$	$\delta_e^2$	$\tilde{D}_c$	$C_{M_\alpha}$ [ $M_\infty = 2.6$ ]*	$C_{M_{\alpha 0}}$ [ $M_\infty = 2.6$ ]**
1 (D)	2.61	.0183	.0043	3.35	.0489	.193	3.36	3.54
2 (D)	2.61	.0184	.0042	3.30	.0496	.186	3.31	3.49
3 (D)	2.60	.0188	.0039	3.15	.0693	.183	3.15	3.41
4 (D)	2.61	.0188	.0042	3.35	.0357	.181	3.36	3.49
5 (D)	2.61	.0186	.0040	3.17	.0536	.181	3.18	3.38
8 (S)	2.61	.0189	.0038	3.09	.0496	.103	3.10	3.28
9 (S)	2.61	.0185	.0041	3.24	.0427	.119	3.25	3.41
10 (S)	2.61	.0191	.0036	2.97	.0415	.096	2.98	3.13
11 (S)	2.61	.0190	.0038	3.06	.0627	.105	3.07	3.30
12 (S)	2.61	.0187	.0036	2.90	.0409	.103	2.91	3.06

All rounds were fired in October 1943 (Hitchcock 1943)

(D) Indicates dense distribution of cards

(S) Indicates sparse distribution of cards

\*  $C_{M_\alpha}$  corrected to  $M_\infty = 2.6$  using  $\frac{\partial C_{M_\alpha}}{\partial M_\infty} = -0.64$

\*\*  $C_{M_\alpha}$  corrected to zero yaw using  $C_2 = -3.7$

**Table 4. Yaw-Card Data for the 20MM T215E1 Projectile.**

Round Number	Mach Number	$\phi'_1$ (rad/cal)	$\phi'_2$ (rad/cal)	$C_{M_\alpha}$	$\delta_c^2$	$\bar{D}_c$	$C_{M_\alpha}$ [ $M_\infty = 2.6$ ]*	$C_{M_{\alpha_0}}$ [ $M_\infty = 2.6$ ]**
2 (D)(a)	2.58	.0192	.0039	3.18	.0093	.169	3.17	3.26
5 (D)	2.59	.0197	.0039	3.15	.0031	.156	3.14	3.17
6 (D)	2.58	.0195	.0037	3.00	.0090	.158	2.99	3.07
7 (D)	2.59	.0199	.0037	3.08	.0048	.137	3.07	3.11
8 (S)	2.59	.0196	.0031	2.56	.0071	.064	2.55	2.62
9 (S)	2.59	.0201	.0031	2.60	.0145	.052	2.59	2.72
10 (S)	2.59	.0201	.0029	2.42	.0138	.060	2.41	2.54
11 (S)	2.58	.0207	.0031	2.68	.0160	.081	2.67	2.82
2 (S)(b)	2.61	.0198	.0033	2.71	.0090	.070	2.72	2.80
5 (S)	2.61	.0197	.0032	2.65	.0062	.070	2.66	2.72
6 (S)	2.61	.0197	.0031	2.61	.0124	.064	2.62	2.74
8 (D)	2.60	.0190	.0039	3.02	.0071	.168	3.02	3.09
9 (D)	2.61	.0191	.0038	2.92	.0064	.170	2.93	2.99
10 (D)	2.61	.0189	.0041	3.16	.0062	.176	3.17	3.23

(a) Rounds fired in May 1951 (Hitchcock 1953)

(b) Rounds fired in October 1952 (Hitchcock 1953)

(D) Indicates dense distribution of cards

(S) Indicates sparse distribution of cards

\*  $C_{M_\alpha}$  corrected to  $M_\infty = 2.6$  using  $\frac{\partial C_{M_\alpha}}{\partial M_\infty} = -0.55$

\*\*  $C_{M_\alpha}$  corrected to zero yaw using  $C_2 = -9.3$

Table 5. Yaw-Card Data for the 90MM M71 Shell.

Round Number	Mach Number	$\phi'_1$ (rad/cal)	$\phi'_2$ (rad/cal)	$C_{M_\alpha}$	$\delta_e^2$	$\tilde{D}_c$	$C_{M_\alpha}$ [ $M_\infty = 2.4$ ]*	$C_{M_{\alpha_0}}$ [ $M_\infty = 2.4$ ]**
1 (D)	2.36	.0157	.0058	3.81	.0288	.189	3.79	3.93
3 (D)	2.37	.0155	.0057	3.70	.0340	.161	3.68	3.84
4 (D)	2.37	.0156	.0059	3.81	.0188	.161	3.79	3.88
5 (D)	2.37	.0159	.0056	3.72	.0380	.156	3.70	3.88
6 (S)	2.37	.0156	.0054	3.53	.0380	.112	3.51	3.69
7 (S)	2.36	.0159	.0054	3.57	.0249	.096	3.55	3.67
8 (S)	2.35	.0162	.0054	3.63	.0259	.090	3.60	3.72
9 (S)	2.36	.0158	.0055	3.65	.0176	.085	3.63	3.71
10 (S)	2.35	.0158	.0053	3.48	.0180	.087	3.45	3.53

All rounds were fired in June 1941 (Hitchcock 1941)

(D) Indicates dense distribution of cards

(S) Indicates sparse distribution of cards

\*  $C_{M_\alpha}$  corrected to  $M_\infty = 2.4$  using  $\frac{\partial C_{M_\alpha}}{\partial M_\infty} = -0.52$

\*\*  $C_{M_\alpha}$  corrected to zero yaw using  $C_2 = -4.7$

Table 6. Comparison of Yaw-Card and Spark Range Results.

Projectile	Mach Number	$C_{M_{\alpha 0}}$ (Yaw Cards)	$C_{M_{\alpha 0}}$ (Spark Range)	$C_2$ (Yaw Cards)	$C_2$ (Spark Range)	$C_{M_{\alpha C}}$ (Yaw Cards)
Cal. .30 Ball M1	2.5	2.37	2.39	-1.5*	-4.7	1.9
Cal. .50 API M8	2.6	2.91	2.90	-3.7	-2.4	3.1
20MM T215E1	2.6	2.43	2.40	-9.3	----	4.3
90MM M71	2.4	3.39	3.31	-4.7	-4.2	2.9

\* This value of  $C_2$  was poorly determined. The spark range value,  $C_2 = -4.7$ , was used to correct  $C_{M_{\alpha 0}}$  to zero yaw.

Table 7. Standard Deviations in  $C_{M_{\alpha}}$ .

Projectile	Mach Number	$\sigma_{C_{M_{\alpha 0}}}$ (Yaw Cards)	$\sigma_{C_{M_{\alpha}}}$ (Spark Range)
Cal. .30 Ball M1	2.5	0.13	0.03
Cal. .50 API M8	2.6	0.10	0.04
20MM T215E1	2.6	0.10	0.03
90MM M71	2.4	0.06	0.02



## 11. REFERENCES

- Boyer, E.D., "Aerodynamic Properties of the 90mm HE M-71 Shell." BRL-MR-1475, U.S. Army Ballistic Research Laboratory, Aberdeen Proving Ground, MD, April 1963. (AD 411804)
- Braun, W.F., "The Free Flight Aerodynamics Range." BRL R-1048, U.S. Army Ballistic Research Laboratory, Aberdeen Proving Ground, MD, July 1958. (AD 202249)
- Fowler, R.H., E.G. Gallop, C.N.H. Lock and H.W. Richmond, "The Aerodynamics of a Spinning Shell." Philosophical Transactions of the Royal Society of London, Series A, Volume 221, 1920.
- Fowler, R.H. and C.N.H. Lock, "The Aerodynamics of a Spinning Shell - Part II." Philosophical Transactions of the Royal Society of London, Series A, Volume 222, 1922.
- Hitchcock, H.P., "Resistance and Stability of Projectiles: Experimental Methods and Details of Computation." BRL Report No. X-113, U.S. Army Ballistic Research Laboratory, Aberdeen Proving Ground, MD, December 1932.
- Hitchcock, H.P., "Stability of 90mm Shell T8." BRL R-236, U.S. Army Ballistic Research Laboratory, Aberdeen Proving Ground, MD, June 1941. (AD 702888)
- Hitchcock, H.P., "Aerodynamics of Small Arms Bullets." BRL R-276, U.S. Army Ballistic Research Laboratory, Aberdeen Proving Ground, MD, May 1942. (AD 491851)
- Hitchcock, H.P., "Yaw and Drift of Caliber 0.50 Bullet, API, M8." BRL-MR-256, U.S. Army Ballistic Research Laboratory, Aberdeen Proving Ground, MD, December 1943. (AD 492746)
- Hitchcock, H.P., "Stability of 20mm HE Shell T215E1 and T215E2." BRL-MR-655, U.S. Army Ballistic Research Laboratory, Aberdeen Proving Ground, MD, March 1953. (AD 008914)
- Hunsaker, J.C. and B.G. Rightmire, "Engineering Applications of Fluid Mechanics." New York: McGraw-Hill Book Company, Inc., 1947.
- Karpov, B.G., "A Comparison of Aerodynamic Data Obtained by 'Yaw Card' and Spark Photography Methods." BRL-MR-728, U.S. Army Ballistic Research Laboratory, Aberdeen Proving Ground, MD, October 1953. (AD 24217)
- Kittyle, R.L., J.D. Packard and G.L. Winchenbach, "Description and Capabilities of the Aeroballistic Research Facility." AFATL-TR-87-08, U.S. Air Force Armament Laboratory, Eglin Air Force Base, FL, May 1987.
- Mann, F.W., "The Bullet's Flight From Powder to Target ." New York: Munn and Co., Publishers, 1909. (Reprinted 1942, 1952.)
- McCoy, R.L., "The Aerodynamic Characteristics of 7.62mm Match Bullets." BRL-MR-3733, U.S. Army Ballistic Research laboratory, Aberdeen Proving Ground, MD, December 1988. (AD 205633)

- McCoy, R.L., "The Aerodynamic Charactersitics of .50 Ball, M33, API, M8, and APIT, M20 Ammunition." BRL-MR-3810, U.S. Army Ballistic Research Laboratory, Aberdeen Proving Ground, MD, January 1990. (AD 219106)
- Murphy, C.H., "Free Flight Motion of Symmetric Missiles." BRL-R-1216, U.S. Army Ballistic Research Laboratory, Aberdeen Proving Ground, MD, July 1963. (AD 442757)
- Rogers, W.K., "The Transonic Free Flight Range." BRL-R-1044, U.S. Army Ballistic Research Laboratory, Aberdeen Proving Ground, MD, June 1958. (AD 200177)
- Wylie, C.R., Jr., "Advanced Engineering Mathematics." Second Edition, New York: McGraw-Hill Book Company, Inc., 1960.

## LIST OF SYMBOLS

<u>Symbol</u>	<u>Definition</u>	
$a_0$	=	constant in Fourier series expansion
$a_n$	=	Euler coefficient in Fourier series expansion
$C_2$	=	cubic overturning moment coefficient
$C_{D_c}$	=	$\frac{\pm   \text{Card Drag Force}  }{[(\pi/4) \rho_c d \tau_c V^2]}$
$C_{M_\alpha}$	=	$\frac{\pm   \text{Overturning Moment}  }{[(1/2) \rho V^2 S d \delta]}$ Positive coefficient: Moment increases total angle of attack, $\alpha_t$
$C_{M_{\alpha_c}}$	=	$\frac{\pm   \text{Card Overturning Moment}  }{[(\pi/4) \rho_c d^2 \tau_c V^2 \delta]}$ Positive coefficient: Moment increases total angle of attack $\alpha_t$ .
$C_{N_{\alpha_c}}$	=	$\frac{\pm   \text{Card Normal Force}  }{[(\pi/4) \rho_c d \tau_c V^2 \delta]}$ Positive coefficient: Force in plane of total angle of attack, $\alpha_t$ , $\perp$ to missile axis, in direction of $\alpha_t$ .
$C_{M_{\alpha_0}}$	=	zero-yaw overturning moment coefficient
$d$	=	projectile reference diameter
$\bar{D}_c$	=	$\left[ \left( \frac{\rho_c}{\rho} \right) \left( \frac{\tau_c}{d} \right) \left( \frac{2}{S_c} \right) \right],$ effective card density
$F_{D_c}$	=	card drag force
$F_{N_c}$	=	card normal force

<u>Symbol</u>	<u>Definition</u>
$I(s)$	= unit pulse function
$I_x$	= axial moment of inertia
$I_y$	= transverse moment of inertia
$K_1$	= magnitude of the fast yaw mode
$K_2$	= magnitude of the slow yaw mode
$l$	= interaction distance of projectile with a yaw card (calibers)
$L$	= average yaw period
$M$	= $\frac{\rho S d^3}{2 I_y} C_{M_\alpha}$
$M_c$	= $\frac{\pi \rho_c \tau_c d^4}{4 I_y} C_{M_{\alpha_c}}$
$M_{M_c}$	= card overturning moment
$N_c$	= total number of yaw cards
$p$	= roll rate
$P$	= $\left( \frac{I_x}{I_y} \right) \left( \frac{p d}{V} \right)$
$s$	= arc length along trajectory (calibers)
$S$	= $(\pi d^2/4)$ , reference area
$S_c$	= card spacing (calibers)
$S_g$	= gyroscopic stability factor
$T_n$	= any term in the infinite series of equation (20)

<u>Symbol</u>	<u>Definition</u>
$V$	= projectile speed
$\alpha$	= angle of attack
$\alpha_t$	= $(\alpha^2 + \beta^2)^{\frac{1}{2}} = \sin^{-1} \delta$ , total angle of attack
$\beta$	= angle of sideslip
$\delta$	= $\sin \alpha_t$
$\delta_e^2$	= $K_1^2 + K_2^2 + \frac{\phi'_1 K_1^2 - \phi'_2 K_2^2}{\phi'_1 - \phi'_2}$
$\tilde{\xi}$	$\cong \sin \beta + i \sin \alpha$
$\rho$	= air density
$\rho_c$	= density of yaw card material
$\tau_c$	= thickness of yaw card
$\phi_1$	= $\phi_{1_0} + \phi'_1 s$
$\phi_2$	= $\phi_{2_0} + \phi'_2 s$
$\phi'_1$	= fast mode frequency
$\phi'_2$	= slow mode frequency
$\phi_{1_0}$	= fast mode phase angle
$\phi_{2_0}$	= slow mode phase angle
$\phi'/\pi$	= linear rate of precession
$\hat{\phi}$	= $\phi_1 - \phi_2$

INTENTIONALLY LEFT BLANK.

<u>No. of Copies</u>	<u>Organization</u>	<u>No. of Copies</u>	<u>Organization</u>
2	Administrator Defense Technical Info Center ATTN: DTIC-DDA Cameron Station Alexandria, VA 22304-6145	1	Commander U.S. Army Tank-Automotive Command ATTN: ASQNC-TAC-DIT (Technical Information Center) Warren, MI 48397-5000
1	Commander U.S. Army Materiel Command ATTN: AMCAM 5001 Eisenhower Ave. Alexandria, VA 22333-0001	1	Director U.S. Army TRADOC Analysis Command ATTN: ATRC-WSR White Sands Missile Range, NM 88002-5502
1	Commander U.S. Army Laboratory Command ATTN: AMSLC-DL 2800 Powder Mill Rd. Adelphi, MD 20783-1145	1	Commandant U.S. Army Field Artillery School ATTN: ATSF-CSI Ft. Sill, OK 73503-5000
2	Commander U.S. Army Armament Research, Development, and Engineering Center ATTN: SMCAR-IMI-I Picatinny Arsenal, NJ 07806-5000	2	Commandant U.S. Army Infantry School ATTN: ATZB-SC, System Safety Fort Benning, GA 31903-5000
2	Commander U.S. Army Armament Research, Development, and Engineering Center ATTN: SMCAR-TDC Picatinny Arsenal, NJ 07806-5000	(Class. only) 1	Commandant U.S. Army Infantry School ATTN: ATSH-CD (Security Mgr.) Fort Benning, GA 31905-5660
1	Director Benet Weapons Laboratory U.S. Army Armament Research, Development, and Engineering Center ATTN: SMCAR-CCB-TL Watervliet, NY 12189-4050	(Unclass. only) 1	Commandant U.S. Army Infantry School ATTN: ATSH-CD-CSO-OR Fort Benning, GA 31905-5660
(Unclass. only) 1	Commander U.S. Army Armament, Munitions, and Chemical Command ATTN: AMSMC-IMF-L Rock Island, IL 61299-5000	1	WL/MNME Eglin AFB, FL 32542-5000  <u>Aberdeen Proving Ground</u>
1	Director U.S. Army Aviation Research and Technology Activity ATTN: SAVRT-R (Library) M/S 219-3 Ames Research Center Moffett Field, CA 94035-1000	2	Dir, USAMSAA ATTN: AMXSY-D AMXSY-MP, H. Cohen
1	Commander U.S. Army Missile Command ATTN: AMSMI-RD-CS-R (DOC) Redstone Arsenal, AL 35898-5010	1	Cdr, USATECOM ATTN: AMSTE-TC
		3	Cdr, CRDEC, AMCCOM ATTN: SMCCR-RSP-A SMCCR-MU SMCCR-MSI
		1	Dir, VLAMO ATTN: AMSLC-VL-D
		10	Dir, USABRL ATTN: SLCBR-DD-T

<u>No. of Copies</u>	<u>Organization</u>	<u>No. of Copies</u>	<u>Organization</u>
1	Commander U.S. Army Communications - Electronics Command ATTN: AMSEL-ED Fort Monmouth, NJ 07703-5022	4	Commanding Officer Naval Weapons Support Center ATTN: Code 2021, Bldg. 2521 Mr. C. Zeller ATTN: Code 2022 Mr. R. Henry Mr. G. Dornick Mr. J. Maassen Crane, IN 47522-5020
1	Commander U.S. Army Missile Command ATTN: AMSMI-AS Redstone Arsenal, AL 35898-5000	1	Commanding General MCDEC ATTN: Code D091 Fire Power Division Quantico, VA 22134-5080
2	Air Force Armament Laboratory ATTN: AFATL/FXA Mr. G. Abate Mr. G. Winchenbach Eglin AFB, FL 32542-5000	1	U.S. Secret Service J. J. Rowley Training Center ATTN: Mr. B. Seiler 9200 Powder Mill Road, RD 2 Laurel, MD 20707
1	Director Requirements and Programs Directorate HQ, TRADOC Analysis Command ATTN: ATRC-RP Fort Monroe, VA 23651-5143	1	Commander Naval Surface Warfare Center ATTN: Code G31 Mr. F. Willis Dahlgren, VA 22408-5000
1	Commander TRADOC Analysis Command ATTN: ATRC Fort Leavenworth, KS 66027-5200	1	Tioga Engineering Company ATTN: Mr. W. Davis, Jr. 13 Cone Street Wellsboro, PA 16901
1	Director TRADOC Analysis Command - White Sands Missile Range White Sands Missile Range, NM 88002-5502	1	Mr. Robert B. Lutz 109 Hillside Drive Carlisle, PA 17013
1	Commandant U.S. Army Infantry School ATTN: ATSH-CD-CS-OR Fort Benning, GA 31905-5400		
1	President U.S. Army Infantry Board ATTN: ATZB-IB-SA Mr. L. Tomlinson Fort Benning, GA 31905-5800		
1	Commander Naval Sea Systems Command ATTN: Code 62CE Mr. R. Brown Washington, DC 20362-5101		



<u>No. of Copies</u>	<u>Organization</u>
16	<p>Commander  Armament RD&amp;E Center  U.S. Army AMCCOM  ATTN: SMCAR-SCJ            Mr. J. Ackley            Mr. V. Shisler            Mr. H. Wreden            Mr. J. Hill  ATTN: SMCAR-CCL-AD            Mr. F. Puzycki            Mr. W. Schupp            Mr. R. Mazeski            Mr. D. Conway  ATTN: SMCAR-CCL-FA            Mr. R. Schlenner            Mr. J. Fedewitz            Mr. P. Wyluda  ATTN: SMCAR-SCA-AP            Mr. W. Bunting  ATTN: SMCAR-AET-AP            Mr. R. Kline            Mr. Chiu Ng            Mr. H. Hudgins            Mr. S. Kahn  Picatinny Arsenal, NJ 07806-5000</p>

<u>No. of Copies</u>	<u>Organization</u>
	<p><u>Aberdeen Proving Ground</u>  Director, USAMSAA  ATTN: AMXSY-J            Mr. K. Jones            Mr. M. Carroll            Mr. J. Weaver            Mr. E. Heiss            AMXSY-GI            Mr. L. DeLattre  Commander, USATECOM  ATTN: AMSTE-SI-F  Commander, CRDEC, AMCCOM  ATTN: SMCCR-RSP-A            Mr. M. Miller            Mr. J. Huerta</p> <p>Director, USAHEL  ATTN: SLCHE-IS            Mr. B. Corona            Mr. P. Ellis</p> <p>Director, USACSTA  ATTN: STECS-AS-LA            Mr. G. Niewenhous</p>

INTENTIONALLY LEFT BLANK.

# USER EVALUATION SHEET/CHANGE OF ADDRESS

This laboratory undertakes a continuing effort to improve the quality of the reports it publishes. Your comments/answers below will aid us in our efforts.

1. Does this report satisfy a need? (Comment on purpose, related project, or other area of interest for which the report will be used.) \_\_\_\_\_

2. How, specifically, is the report being used? (Information source, design data, procedure, source of ideas, etc.)

3. Has the information in this report led to any quantitative savings as far as man-hours or dollars saved, operating costs avoided, or efficiencies achieved, etc? If so, please elaborate.

4. General Comments. What do you think should be changed to improve future reports? (Indicate changes to organization, technical content, format, etc.) \_\_\_\_\_

BRL Report Number BRL-TR-3338 Division Symbol

Check here if desire to be removed from distribution list. \_\_\_\_\_

**Check here for address change.** \_\_\_\_\_

Current address: Organization \_\_\_\_\_  
Address \_\_\_\_\_

DEPARTMENT OF THE ARMY

Director  
U.S. Army Ballistic Research Laboratory  
ATTN: SLCBR-DD-T  
Aberdeen Proving Ground, MD 21005-5066

OFFICIAL BUSINESS

**BUSINESS REPLY MAIL**

**FIRST CLASS PERMIT No 0001, APG, MD**

**Postage will be paid by addressee.**

**Director  
U.S. Army Ballistic Research Laboratory  
ATTN: SLCBR-DD-T  
Aberdeen Proving Ground, MD 21005-5066**

NO POSTAGE  
NECESSARY  
IF MAILED  
IN THE  
UNITED STATES